# Study on organic matter fractions in the surface microlayer in the Baltic Sea by spectrophotometric and spectrofluorometric methods

Violetta Drozdowska[1], Iwona Wróbel[1], Piotr Markuszewski[1], Przemysław Makuch[1], Anna Raczkowska[2], Piotr Kowalczuk[2]

[1]Physical Oceanography Department, Institute of Oceanology Polish Academy of Science, Sopot, 81-712, Poland
[2]Marine Physics Department, Institute of Oceanology Polish Academy of Science, Sopot, 81-712, Poland

*Correspondence to:* Violetta Drozdowska (drozd@iopan.pl)

**Abstract.** The fluorescence and absorption measurements of the samples collected from a surface microlayer (SML) and a subsurface layer (SS), a depth of 1 m were studied during three research cruises in the Baltic Sea along with hydrophysical studies and meteorological observations. Several absorption ($E_2$:$E_3$, S, $S_R$) and fluorescence (fluorescence intensities at peaks: A, C, M, T, the ratio (M+T)/(A+C), HIX) indices of colored and fluorescent organic matter (CDOM and FDOM) helped to describe the changes in molecular size and weight as well as in composition of organic matter. The investigation allow to assess a decrease in the contribution of two terrestrial components (A and C) with increasing salinity (~1.64% and ~1.89 % in SML and ~0.78% and ~0.71 % in SS, respectively) and an increase of in-situ produced components (M and T) with salinity (~0.52% and ~2.83% in SML and ~0.98% and ~1.87% in SS, respectively). Hence, a component T reveals the biggest relative changes along the transect from the Vistula River outlet to Gdansk Deep, both in SML and SS, however an increase was higher in SML than in SS (~18.5% and ~12.3%, respectively). The ratio $E_2$:$E_3$ points to greater changes in a molecular weight of CDOM affected by a higher rate of photobleaching in SML. HIX index reflects a more advanced stage of humification and condensation processes in SS. Finally, the results reveal a higher rate of degradation processes occurring in SML than in SS. Thus, the specific physical properties of surface active organic molecules (surfactants) may modify, in a specific way, the solar light spectrum entering the sea and a penetration depth of the solar radiation. Research on the influence of surfactants on the physical processes linked to the sea surface become an important task, especially in coastal waters and in vicinity of the river mouths.

## 1. Introduction

The sea surface is a highly productive and active interface between the sea and the atmosphere. The physicochemical and biological properties of a surface microlayer (SML, a surface film), are clearly and measurably different from the underlying water due to the molecules forming SML, called surfactants (Soloviev and Lukas, 2006; Liss and Duce, 2005). Sea surface films are created by organic matter from sea and land sources: (i) dissolved and suspended products of marine plankton contained in seawater, (ii) terrestrial organic matter that enter seawater from a land (natural and synthetic) and (iii) oil products from leakages of the sea-bottom. Surface films dissipate due to loss of material at the sea surface, including microbial degradation, chemical and photo chemical processes, as well as due to absorption and adsorption

onto particulates (Liss et al., 1997). However the surface microlayer is almost ubiquitous and cover most of the surface of the ocean, even under conditions of high turbulence (Cuncliffe et al., 2013). Surface active molecules (surfactants) present in SML may modify the number of physical processes taking place in the surface microlayer: among others they affect the depth of penetration of solar radiation and gas exchange, e.g. the generation of aerosols from the sea surface (Vaishaya et al., 2012; Ostrowska et al., 2015; Petelski et al., 2014). Therefore, research on the influence of surfactants on the sea surface properties become an important task, especially in coastal waters and in a vicinity of the river mouths (Maciejewska and Pempkowiak, 2015).

Surfactants comprises a mixture of organic molecules rich in lipids (fatty acids, sterols), polymeric and humus which proportions determine the various properties of the SML. Some organic compounds possess the optically active parts of the molecules, i.e. chromophores, that absorb the light energy (CDOM, *chromophoric* dissolved organic matter), and fluorophores, that absorb and emit the light (FDOM). Due to the complexity and variability of the composition of the marine organic matter mixture, the best tool (fast and reliable) to detect and identify the organic matter in seawater is the absorption and fluorescence (excitation-emission matrix) spectroscopy (Stedmon et at, 2003; Hudson et al., 2007; Coble, 2007). A unique structure of the energy levels of these organic molecules results in a specific spectral distribution of the light intensities absorbed and emitted by the molecules. Hence, the absorption and fluorescence spectra of organic compounds may allow the identification of the sources of organic matter (Coble, 1996; Lakowicz, 2006). The analysis of the absorption and 3D fluorescence spectra enabled to calculate several indices describing the changes of a concentration, a molecular weight, a composition of CDOM/FDOM and a rate of degradation processes of the organic matter occurring in the study surface layers.

There are many applications of the absorption and fluorescence spectroscopy in oceanographic studies on mixing water masses locally, e.g. in estuaries (Williams et al., 2010) and in global scale (Jorgensen et al., 2011). The studies were conducted in various natural waters as e.g. Chinese lakes (Zhang et al 2013; Chen et al., 2011), Indian Ocean (Chari et al., 2012), American estuaries (Glatzel et al., 2003; McKnight et al., 1997; Moran et al., 2000) and in studies on dilution sea basins, such as the Baltic (Kowalczuk et al., 2010; Drozdowska et al., 2002) and Arctic (Gueguen et al., 2007) that considered the differences in FDOM components from the rivers, lakes and inland water.

This paper is focus on distinguishing fate and concentration of specific CDOM/FDOM components of organic matter to detect and describe the processes that occur in the sea surface microlayers (SML) and in subsurface layers (SS), a depth of 1 m. Research are based on the absorption and fluorescence spectra and several absorption and fluorescence indices. Investigations concern the region of Gulf of Gdansk, along a transect from the Vistula River outlet (the biggest Polish river) to open sea.

## 2 ~~Methods~~ Measurements

### 2.1 Materials and study area

Research to identify the marine surfactants were conducted during three research cruises of r / y ‘Oceania’ (two cruises in 2015 and one in 2016). The study was conducted at nine stations along the transect 'W' - from the mouth of the Vistula River, W1, along the Gulf of Gdansk to the Gdansk Deep in the open sea, W9. The

study area is under direct influence of the main Polish river system, Vistula, which drains the majority of Poland (Uścinowicz, 2011). The following tasks were performed at every station: (i) measurement of the hydrophysical parameters (CTD), (ii) sampling the seawater from SML and SS, (iii) preparation the samples to the appropriate laboratory tests (filtration and proper maintenance) and (iv) meteorological observations. The SML samples were collected by the metal Garret's net of 500 μm mesh. This technique allows collecting water from the top-layer of an approximately 1 millimeter (Garrett, 1965). In the same places the SS samples from a depth of 1 m were taken by a Niskin bottle. The unfiltered samples were placed into dark bottles and stored at 4°C. During sampling the measurements of temperature and salinity of a surface layer were conducted. Sampling was carried out when the sea state was 1-4 B only, and there were no detectable oil spills. Additionally, the meteorological observations (e.g. recorded wind speed and wind direction and a high of a wave) during sampling, proved to be valuable in the interpretation of extraordinary results. During sampling, in two research cruises, at April in 2015 and September in 2016, the wind speed was almost equally to zero. However, in October in 2015, a northern-west wind was recorded (3-4 B). In October the cruise started after a week-long storm of northerly winds resulting in the influx of water from the open sea and strong mixing of fresh with coastal and sea water. That allows the explanation of the surprisingly low concentrations (typical for a salinity above 7) of organic matter recorded along entirely transect W, even at the vicinity of the mouth of the Vistula River.

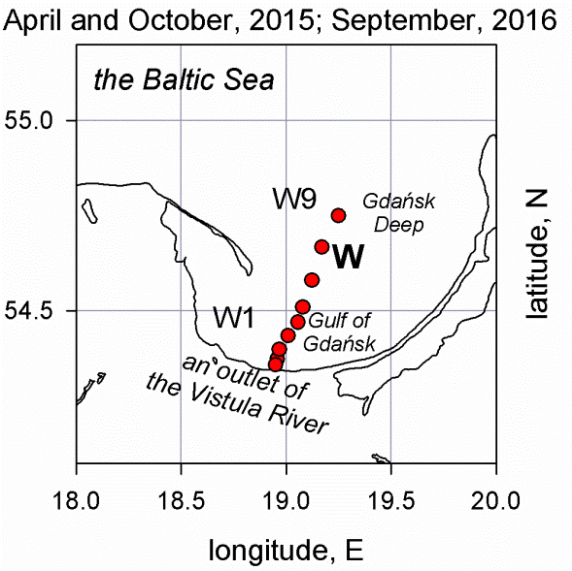


**Figure 1 . Measuring stations realized during research cruises of r/y Oceania: 28th April and 15-16th October in 2015 and 11th September in 2016.**

### 2.2. CDOM and FDOM laboratory measurements.

The studies conducted in laboratory are: (i) measurements of absorption and (ii) 3D fluorescence (EEM) spectra of the surface (SML) and subsurface (SS) samples, from 27 stations. Spectrophotometric and spectrofluorometric measurements of the samples were carried out in 24 hours after collection without any previous treatment at room temperature.

It is well-known that, filtration separates particulate fraction from dissolved and colloidal ones. On the other hand, during filtration the strongly surface active structures of organic molecules or macromolecules might

be retained on the filter by sorption processes (Ćosović and Vojvodić, 1998). Therefore, the all studied samples are analyzed without filtration. Samples for absorption and fluorescence measurements were treated in the same manner.

Absorbance scans, from 240 to 800 nm (1 nm slit width), were conducted using 10 cm cuvette by Perkin Elmer Lambda 650 dual-beam spectrophotometer connected to a PC computer. Milli-Q water was used in the reference cell. Absorbance measurements, $A$, at each wavelength ($\lambda$) were baseline-corrected. CDOM absorption coefficients were calculated by multiplying the corrected optical density by 2.303/$l$, where $l$ is the cuvette path length in meters. The detection limit for the equipment was generally less than 0.002 (so the precision was 0.046 $m^{-1}$ using 10 cm cells).

The 3D steady-state fluorescence spectra (3D EEMs) of the samples, and of Milli-Q water, were carried out using VARIAN Cary Eclipse spectrofluorometer using a 1 cm high sensitivity quartz cell and with 5 nm bandwidth in both excitation and emission, respectively. The excitation of the 3D EEM was fixed in a spectral range 250 – 500 nm, with a step 10 nm. The emission of the 3D EEM was recorded in a spectral range 300 - 600 nm, with a step 2 nm. To make the normalization of 3D EEM spectra, the 3D EEM of Mili-Q water was measured at the beginning of lab measurements every time after the cruise (sampling). Next, the intensity of the Raman emission band as the area, in a range: 374 - 424nm, below the Raman emission curve induced at 350 nm (in literature: 355nm) was calculated (Murphy et al., 2010). Normalization of 3D EEM spectra of the samples, i.e. conversion into Raman units (R.U.), was performed by subtracting the 3D EEM of Milli-Q water from the 3D EEM of the samples and then by dividing the resulting spectra by the respective value of Milli-Q water Raman intensity.

### 2.3 ~~CDOM and FDOM optical properties~~ Optical indices of CDOM and FDOM used for calculations

#### 2.3.1 Absorption indices

Analysis of the absorption spectra enabled to calculate the absorption coefficient, $a_{CDOM}(\lambda)$, (applied as a proxy of CDOM concentration) and several absorption indices. The proposed spectral indices, defined as the ratios of absorption coefficients, are independent on the CDOM concentration, that is very important, because CDOM concentration may vary in a small basin even several times (up to 5-times). The ratios of absorption coefficients at 250 to 365nm (called $E_2$:$E_3$) and at 450 to 650 nm (called $E_4$:$E_5$) are used to track changes in the relative size and the aromaticy of CDOM molecules; briefly, when a molecular size and aromaticy increase, the values of the ratios $E_2$:$E_3$ and $E_4$:$E_5$ decrease. This is caused by the stronger absorption at the longer wavelengths occurring due to the presence of larger and higher molecular weighted (HMW) CDOM molecules (De Haan and De Boer, 1987; Peuravouri and Pihlaja, 1997; Chin et al., 1994; Helms et al., 2008, Summers et al., 1987). However, in many natural waters the absorption at 664 nm is often little or immeasurable and then the absorption at 254 nm (or 280 nm) is used in lieu of the $E_4$:$E_6$ ratio as an indicator of humification or aromaticy (Summers et al., 1987). The next parameter is the absorption spectral slope coefficient, S, calculated as follow:

$$a_\lambda = a_{ref}\, e^{-S(\lambda-\lambda ref)} + K \qquad (1)$$

where $a$ – absorption coefficient, $m^{-1}$, $\lambda$ – wavelength (nm), $S$ – absorption spectral slope ($nm^{-1}$) and K – a background constant, arising from residual scattering or attenuation by not chromophoric organic matter. The spectral slope coefficient, S, of the absorption spectra, calculated in various spectral windows (Carder et al., 1989; Blough and Green, 1995) is used as a proxy for CDOM composition, including the ratio of fulvic to humic acids and molecular weight (Stedmon and Markager, 2003; Bracchini at al., 2006). The use of S in the narrow spectral range allows to reveal subtle differences in the shape of the spectrum and this in turn gives insight into the origin of organic matter (Sarpal et al., 1995). Therefore to calculate the slopes of the absorption spectra the smaller and more discrete spectral ranges are used as they show a great variability depending on the origin of marine CDOM (marsh, riverine, estuarine, coastal and open sea). The use of narrow wavelength intervals is advantageous as they minimize variations in *S* caused by dilution (Brown, 1977). The ratio of the spectral slope coefficients ($S_{275-295}$ and $S_{350-400}$), $S_R$, is related to DOM molecular weight (MW) and to photochemical induced shifts in MW that consistently increased upon irradiation and suggested they are potential indicators of photobleaching in the marine environment (Helms et al., 2008; Zhang et al., 2009, Loiselle et al., 2009). The slope of the absorption curve in the 300-600 nm range, (S), is calculated by fitting the exponential function to the expression (1) over a respective spectral window. While the slope coefficients in the ranges 275-295 nm, ($S_{275-295}$), and 350-400, ($S_{350-400}$), are fitted linearly in two narrower wavelength windows. The steeper slope coefficient (higher values of S) means a faster decrease in absorption with increasing wavelength. A spectral slope coefficient ratio, $S_R$, ($S_{\sout{274}\ 275-295}$ to $S_{350-400}$) is negatively correlated with molecular weight of CDOM in humic substances. The relationship between $S_R$ and molecular weight is very useful to explain the observed variations in $S_R$ caused by aerobic activity or by photobleaching of CDOM (Helms et al., 2008). It was reported that the photochemical degradation of terrestrial DOM generally causes an increase in the absolute value of the spectral slope coefficient, while biological degradation did not affect the spectral slope coefficient, or unless DOM molecules had undergone photo-degradation process, it causes a decrease of a spectral slope coefficient. Hence, the simultaneous photo- and biodegradation processes may compensate their effects on the spectral slope coefficient values (Moran et al., 2000).

### 2.3.2 Fluorescence indices

Analysis of 3D EEM fluorescence spectra of marine waters are based on interpretation of distinct fluorescence intensity peaks proposed first time by Coble (1996) for different types of natural waters, where A is the terrestrial humic substances peak, C the terrestrial fulvic substances peak, M the marine fulvic substances peak and T the proteinaceous peak. The recognized positions (energies) of excitation and emission wavelengths (in: nm/nm) of the main components (A, C, M, T) of marine FDOM at the 3D spectrum, for the Baltic Sea, are: 250/437, 310/429, 300/387 and 270/349, respectively; $\Delta\lambda_{em}$=+/-5 nm, (Kowalczuk et al., 2005; Drozdowska et al., 2015). Based on the 3D (EEM) fluorescence spectra several indices are calculated. The fluorescence intensities of the main FDOM components: A, C, M and T (in Raman units, R.U.) are used as a proxy of FDOM concentration. A percentile contribution of the main FDOM fluorophores, calculated as the ratio of the respective peak intensity (A, C, M or T) to the sum (A+C+M+T) of all peak intensities, gives information about the relative changes of a fluorophore composition in a sample (Kowalczuk et al., 2005; Drozdowska and Józefowicz, 2015). Another fluorescence

indices are the ratio (M+T)/(A+C) (Parlanti et al., 2000) and HIX index. The ratio (M+T)/(A+C) (Drozdowska et al., 2013) allows assessing a relative contribution of the organic matter recently produced, in-situ, (M+T) in the sea to molecules characterized by highly complex structure (A+C) ); the values > 1 indicate the predominant amount of autochthonous DOM molecules, while < 0.6 indicate the allochthonous ones. HIX index is calculated as a ratio of fluorescence intensity at a long wavelength part (435-480) of the fluorescence spectrum (induced in 255nm) to a short wavelength band (330–346 nm) (Chen et al., 2011; Zsolnay et al., 1999; Milori et al., 2002). HIX index reflects the structural changes that occur in the process of humification, causing an increase in both aromaticy (the ratio C/H) and molecular weight of DOM molecules. The applied indices enable to evaluate a relative contribution of the organic matter recently produced, in-situ, in the sea (M and T / an intensity of a short-wavelength fluorescence band) and the molecules characterized by a highly complex structure (A and C / an intensity of a long-wavelength fluorescence band). Thus, the applied indices allow you to assess whether the allochthonous (terrestrial, aromatic and highly weighted molecules) or autochthonous (marine humic-like and protein-like and low molecular weighted ones) organic matter predominate (Chari et al., 2012).

## 3 Results

### 3.1. Absorption analysis

Analysis of the absorption spectra enabled to calculate the absorption coefficients. The absorption at 254 nm exhibits the greater sensitivity to salinity changes than other wavelengths and will be applied as a proxy of CDOM concentration. Fig. 2. presents the absorption spectra, for the nearest-shore, W1, and the most off-shore, W9, stations.

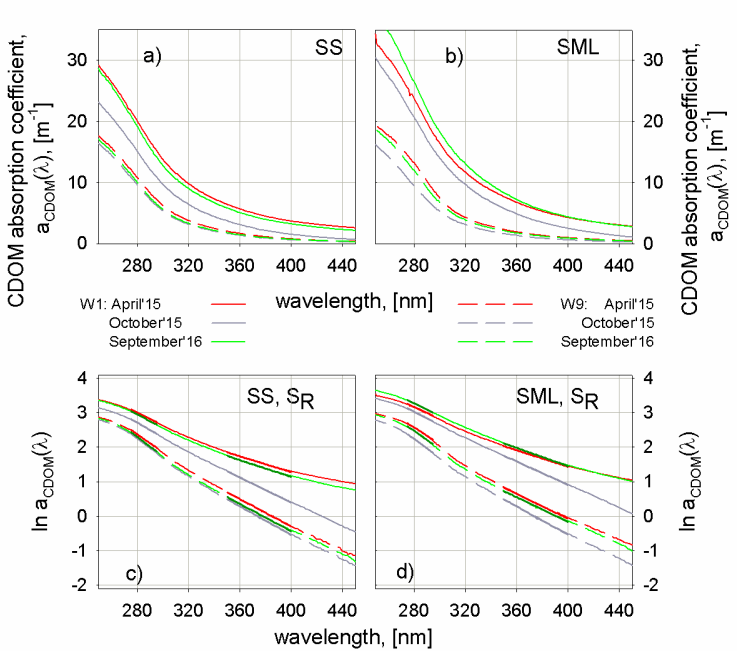


**Figure 2. Absorption spectra - collected during three Baltic cruises at 28th April, 2015 (red lines), 15-16th October, 2015 (grey) and 11th September 2016 (green) - for W1 (solid lines) and W9 (dash lines) stations – presented in linear scale (top panels: a, b). Natural log-transformed absorption spectra with best-fit regression lines for two regions (275-295 nm and 350-400 nm) (bottom panels: c, d).**

The absorption spectra present the typical distribution of the values of the absorption coefficients that decrease exponentially with increasing the wavelengths in a spectral range from UV to visible light. The values of the absorption coefficient, $a_{CDOM}(\lambda)$ are the highest in the station W1, located in the vicinity of a river outlet, and the lowest in W9, in the open sea. Moreover, with an increase of a distance from the river outlet, the intensity of light absorption is decreasing significantly and the differences between the SML and SS ~~become smaller and smaller~~ decrease. Furthermore, the slope ratio $S_R$ , as a ratio of spectral slope coefficients in two spectral ranges of the absorption spectra, $S_{275-295}$ and $S_{350-400}$, was calculated. The sections of the absorption curves, marked in the appropriate narrow spectral ranges and, corresponded to them, the values of $S_R$ are presented in Fig. 2 (c and d) and Table 1, respectively.

Table 1. Results of a slope ratio, $S_R$, for SML and SS, at W1 and W9 stations.

| | A slope ratio – $S_R$ (= $S_{275-295}/S_{350-400}$) | | | | | |
|---|---|---|---|---|---|---|
| | $S_R$ - for SS | | | $S_R$ - for SML | | |
| | ~~28th IV 2015~~ 28 April 2015 | ~~15-16th X 2015~~ 15-16 October 2015 | ~~11th IX 2016~~ 11 September 2016 | ~~28th IV 2015~~ 28 April 2015 | ~~15-16th X 2015~~ 15-16 October 2015 | ~~11th IX 2016~~ 11 September 2016 |
| W1 | 1.58 | 1.16 | 1.61 | 1.43 | 1.10 | 1.35 |
| W9 | 1.30 | 1.33 | 1.40 | 1.34 | 1.35 | 1.45 |

The values of $S_R$ obtained in three cruises at W1 station (near the Vistula River outlet) were: 1.58, 1.16 and 1.61 for SS and 1.43, 1.10 and 1.35 for SML, respectively. While at W9 (open sea) were: 1.30, 1.33 and 1.40 for SS and 1.34, 1.35 and 1.45 for SML, respectively. Hereof, the slope ratio, $S_R$, was higher in SML than in SS in the open sea (W9), while it was opposite in a region around the Vistula river mouth (W1). However in ~~W1~~ W9 (the open sea) the differences were 3.1, 1.5 and 3.5 %, while in W9: 10.5, 5.4 and 11.9 %.

Next, another absorption indices that describe the changes of molecular size/weight (the $E_2$:$E_3$ ratio) and chemical composition of organic matter (a spectral slope coefficient, S), were calculated. The results of $E_2$:E3 and S and $S_R$ in a relation to salinity are presented on Fig. 3. The satisfying correlation between salinity and (i) the spectral slope coefficient, *S* ($r^2$=0.84 for SS and $r^2$=0.67 for SML), (ii) the slope ratio $S_R$ ($r^2$=0.58 for SS and SML) and (iii) relative changes in the molecular weight MW ($r^2$=0.94 for SS and $r^2$=0.57 for SML) were received. Moreover, the linear regression coefficients for the relations between salinity and: S, $S_R$ and MW are, respectively 0.00439, 0.13 and 3.029 for SML and 0.00435, 0.11 and 2.293 for SS. As one can see, the linear regression coefficients achieved higher values for SML than SS, so the processes go faster in SML than in SS.

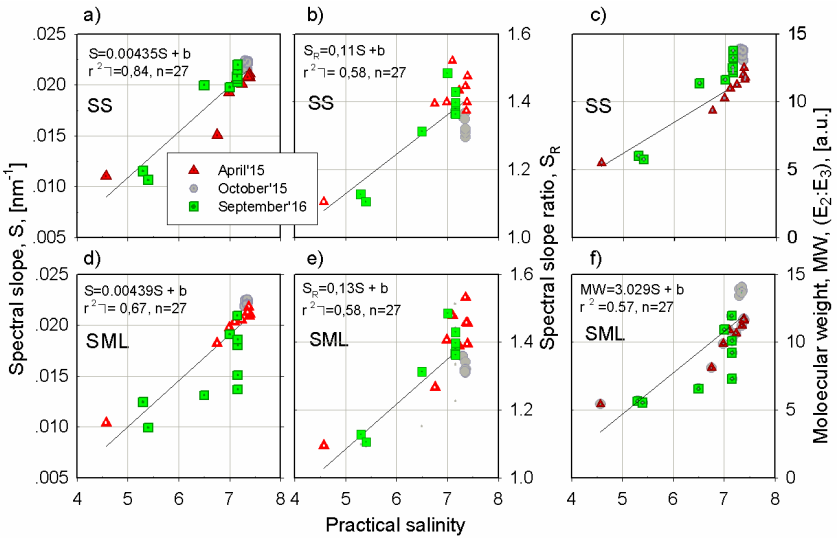


**Fig. 3. The relationship between salinity and: (a) the spectral slope coefficient, S, measured in the 300-600nm, (b) the slope ratio $S_R = S_{275-295} / S_{350-400}$, and (c) the relative changes in the molecular weight, MW ($E_2$: $E_3$) for SS; and: (d), (e) and (f) for SML, respectively.**

Furthermore, the values of S, $S_R$ and MW are 2-, 0.5- and 3-times higher, respectively, in a vicinity of the river outlet than in open sea.

### 3.2 Fluorescence analysis

Based on the analysis of 54 EEM spectra of seawater (27 samples for SML and 27 ones for SS) the intensities of four emission bands (in R.U.), belonging to the main components (A, C, M and T) of the marine CDOM were calculated. The Fig. 4 presents the 3D EEM spectra, typical for the open sea water (the most salty) , W9, and estuarine waters (the most fresh), W1, for the samples collected from SML and SS.

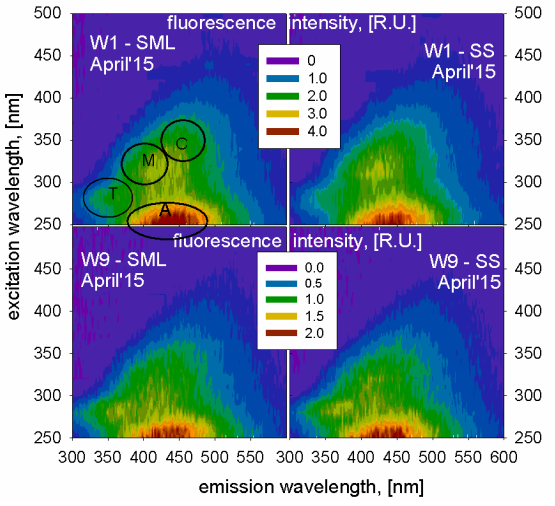


**Figure 4. Examples of 3D fluorescence spectra (EEM) of the samples collected at stations W1, near the Vistula River outlet (top panels) and W9, Gdansk Deep (bottom panels), 28 April 2015.**

The relationships between the fluorescence intensities of the main fluorescence bands (proxy of FDOM components concentration) and salinity as well as the relative contribution of the fluorescent components and salinity are demonstrated in Fig. 5 and 6. The changes of the FDOM peak intensities and their relative contributions (composition of FDOM components) in EEM were quantify by calculating the median and its

percentile distribution of both the fluorescence intensities and the relative contributions of FDOM components, for the SML and SS in two water masses. Table 2 contains the median values of (i) fluorescence intensities (R.U.) and (ii) percentage contribution (%) of respective peaks in the SML and SS in two distinct water masses: one characterized by salinity <7, which is influenced by direct fresh water discharge from Vistula River and the other characterized by salinity >7, which is typical for open Baltic Sea waters.

The fluorescence intensities of the main FDOM components referred to salinity demonstrate the constant linear relationships both in SS and SML (Fig. 5, upper and lower graphs, respectively). The linear regression coefficients in SML and SS, for every FDOM component, are: -1.43 and -1.02 for a component A; -0.84 and -0.65 for a component C; -0.56 and -0.43 for a component M; -0.32 and -0.3 a component T, respectively. Hence, the regression coefficients are higher in SML than in SS.

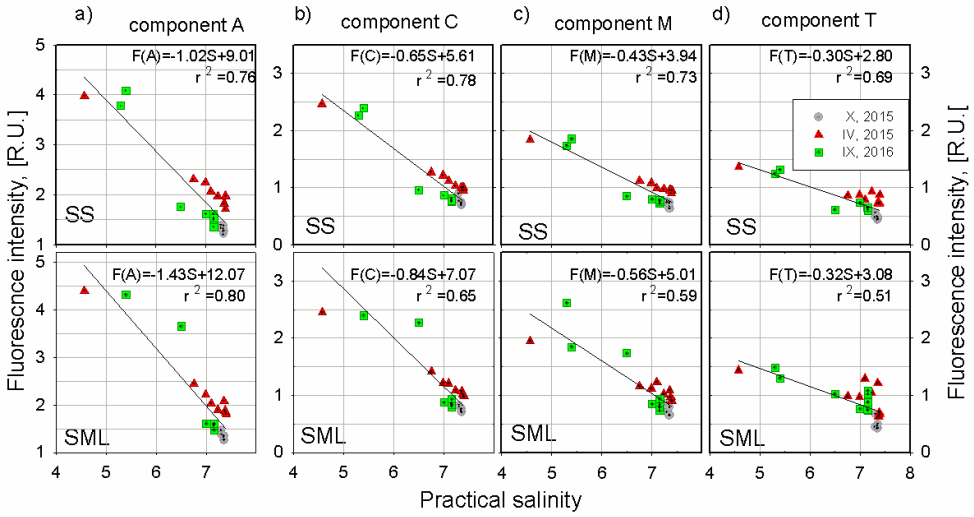


**Figure. 5. Dependence of the fluorescence intensity of the main FDOM components: a) A, b) C, c) M and d) T as a linear relation to salinity for the samples from the sub-surface water (SS; top panels) and the sea surface microlayer (SML; bottom panels).**

Table 2. Medians of FI* and PC** of FDOM components for coastal zone*** and open sea waters****

| | | | Salinity < 7 | | | | Salinity > 7 | | | |
|---|---|---|---|---|---|---|---|---|---|---|
| FDOM components | | | A | C | M | T | A | C | M | T |
| exc./ em. (nm/nm) | | | 250/437 | 310/429 | 300/387 | 270/349 | | | | |
| fluorescence intensity, R.U. | median | SML | 2.69 | 2.27 | 1.74 | 0.98 | 1.56 | 0.84 | 0.85 | 0.69 |
| | | SS | 2.31 | 1.27 | 1.12 | 0.86 | 1.50 | 0.77 | 0.76 | 0.63 |
| percentile contribution, % | median | SML | 40.72 | 24.32 | 20.01 | 14.06 | 39.08 | 22.43 | 20.53 | 16.89 |
| | | SS | 41.52 | 22.87 | 19.92 | 14.40 | 40.75 | 22.17 | 20.90 | 16.27 |

*FI - a fluorescence intensity; **PC - a percentage contribution; ***typical for salinity < 7; ****typical for salinity > 7.

The percentile statistical distribution of fluorescence peak intensities in the SML and SS layer in two water masses characterized by salinity threshold less that 7 and higher than 7, have been presented in Fig. 6a and Fig.6b, respectively. The box-whisker plots in Fig. 6 present median values (solid line), 25th and 75th

percentile (the boundaries of the box: closest to and farthest from zero, respectively) and 5th and 95th percentiles (whiskers below and above the box, respectively) of the respective fluorescence intensity. There has been a clear spatial pattern (for the coastal zone and open sea) shown on both figures that the higher median values of A, C, M and T were observed in the SML than in SS. For salinity <7, the median of fluorescence intensities of main FDOM components in SML were: 2.69, 2.27, 1.74 and 0.98 R.U., while in SS: 2.31, 1.27, 1.12 and 0.86 R.U. In open waters (salinity >7) the median of fluorescence intensities of the FDOM components were in SML: 1.56, 0.84, 0.85 and 0.69 R.U., while in SS: 1.5, 0.77, 0.76 and 0.63 R.U. The median values of respective peaks intensities are higher in SML than in SS both in coastal zone (salinity <7) and in open sea (salinity >7). Additionally, the boundaries of the boxes show much greater dispersion of the results in SML than in SS and greater variation in coastal zone (salinity <7) than in open sea (salinity >7).

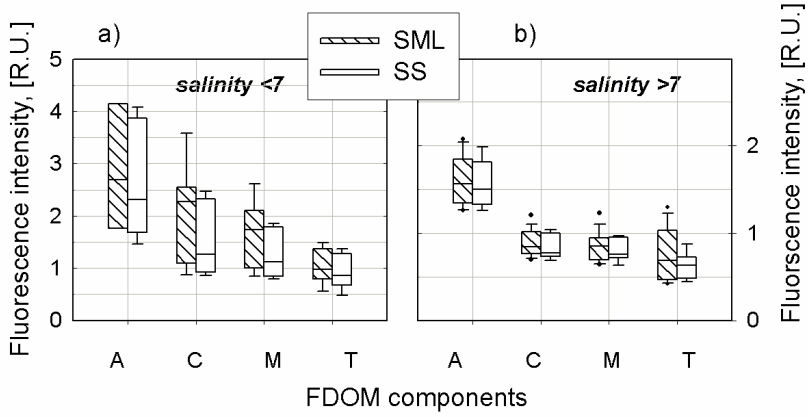


**Figure 6. Dependence of the fluorescence intensity of the main FDOM components in SML and SS as the box plots for (a) coastal water (salinity <7) and (b) open sea (salinity >7).**

The Fig. 7 shows the percentage contribution of the individual FDOM peaks calculated as the ratio of its fluorescence intensity to the sum of the all fluorescence peak intensities (e.g. A/(A+C+M+T)) for SS and SML samples (a left and a right graph, respectively). The box-whisker plots in Fig. 7 present median values (solid line), 25th and 75th percentile (the boundaries of the box: closest to and farthest from zero, respectively) and 5th and 95th percentiles (whiskers below and above the box, respectively) of the respective percentage contribution (a relative composition of fluorescing components of CDOM).

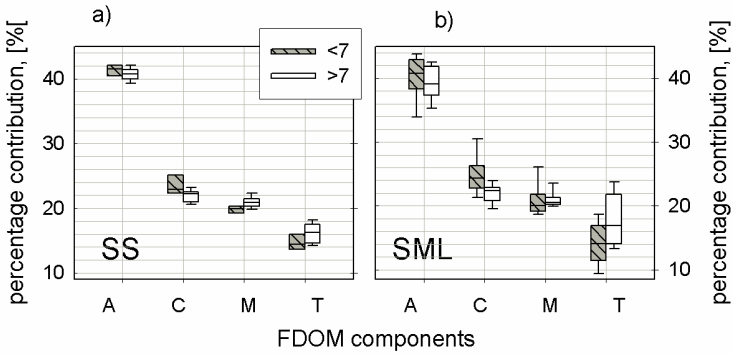


**Figure. 7. Dependence of percentage contribution of the main FDOM components as the box plots for (a) the sub-surface water, SS and (b) the sea surface microlayer, SML; for the coastal waters (salinity <7) and open sea (salinity >7).**

For salinity <7, the medians of percentage contribution of A, C, M and T components of marine FDOM in SML were: 40.72%, 24.32%, 20.01% and 14.06 % while in SS: 41.52%, 22.87, 19.92 and 14.40 %,

respectively. In open waters (salinity >7) the median values of FDOM components composition were in SML 39.08, 22.43, 20.53 and 16.89 % while in SS: 40.75, 22.17, 20.90 and 16.27 %. So, the contribution of two terrestrial components (A and C) decreased with increasing salinity (~1.64% and ~1.89 % in SML and ~0.78% and ~0.71 % in SS, respectively), while the contribution of, in-situ, in the sea produced components (M and T) increased with salinity (~0.52% and ~2.83% in SML and ~0.98% and ~1.87 % in SS, respectively), Fig. 7. Considering the aforementioned changes for an individual component in relation to its percentage contribution, the values of their relative changes can be calculated. Hereby, the ~~biggest~~ highest relative changes of the FDOM component composition, along the transect from the Vistula River outlet to Gdansk Deep, were recorded for component T, both in SML and SS (about 18.5 % and ~12.3 %, respectively), while the relative changes of A, C and M components were: 4.1, 8.1 and 2.6 % in SML and 1.9, 3.1 and 4.7 % in SS, respectively.

The values of peak intensities (A, C, M and T) allowed to calculate (i) the ratio (M+T)/(A+C) and (ii) index HIX in SML and SS water, presented on Fig. 8.

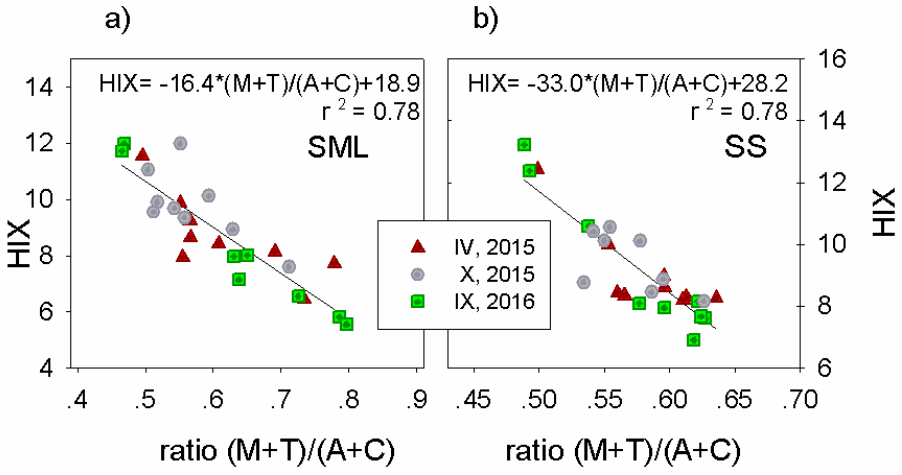


**Figure 8. The relationship between the ratio (M+T)/(A+C) and HIX index for (a) SML and (b) SS water.**

The low values of the ratio (M + T)/(A + C), (<~0.6), were recorded in almost all samples from a sub-surface layer, SS, while in SML samples only from the Gulf of Gdansk. The results of the ratio varied along the transect W in the range 0.47 to 0.79 for SML and 0.49 to 0.63 for SS, from W1 to W9 respectively. Thus, the ratio describes the process that occurs more effectively in SML. The results of the index HIX achieved the higher values in the SS than in SML. What is more, the HIX index changed in SML in a range: 5.8 – 11.9 while in SS: 6.9 – 13.2. The elevated values of HIX in the SS indicate a presence of the molecules of higher molecular weight and more condensed, with higher aromaticy, than in SML, Fig. 8.

### 3.3 The absorption and fluorescence dependences.

The absorption and fluorescence results allow comparing the spectral slope ratio, $S_R$, with the HIX index and the ratio $E_2$:$E_3$ to find the dependences of the molecular size/weight in SML and SS with condensation degree of organic molecules and with the changes in chemical composition of organic matter, Fig. 9. High values of HIX index coincide with low values of $S_R$. While $S_{275-295} < S_{350-400}$ means the occurrence and predominance of highly condensed matter and/or terrestrial DOM, with HMW molecules absorbing in a long wavelength range. Whereas, the lower HIX and higher $S_R$ values ($S_{275-295} > S_{350-400}$) mean the predominance of marine-

derived, LMW molecules absorbing in a short wavelength range. The relation between HIX index and $S_R$ show a simple linear relation in sub-surface waters, SS. However in the sea surface microlayer, SML, the changes in organic matter composition, $S_R$, are not linear-related with the changes taking place in DOM molecules undergoing the degradation processes reflected by HIX values. HIX index is sensitive to the humification and condensation processes, focused on large, high weighted organic molecules, that reflect the changes in a long-wavelength range mainly (above 330 nm). However the photochemical degradation processes, resulting in a decrease in the mass of molecules and an increase of concentration of low molecular-weighted molecules, are much more spectacular in a ~~shorter~~ lower wavelength range and are held primarily in the surface microlayer, SML. For the same reason as was mentioned above, the relation between the ratio $E_2$:$E_3$ and $S_R$ is better correlated in SML than SS water. Moreover, the relation between the $E_2$:$E_3$ and $S_R$ (both inversely proportional to molecular size and weight) shows more discrete differences in molecular structure of the organic molecules studied in different seasons and allows to note the different nature of the water tested in October'2015. The values of the ratio $E_2$:$E_3$ (inversely proportional to molecular size and weight of molecules), calculated for the data collected in October'2015, point to the extremely small size as well as almost the same size/weight of organic molecules investigated in the entirely study region both in SML and SS. That confirms a very well mixed water and the surface layer in the study area, suggested previously by the meteorological observations.

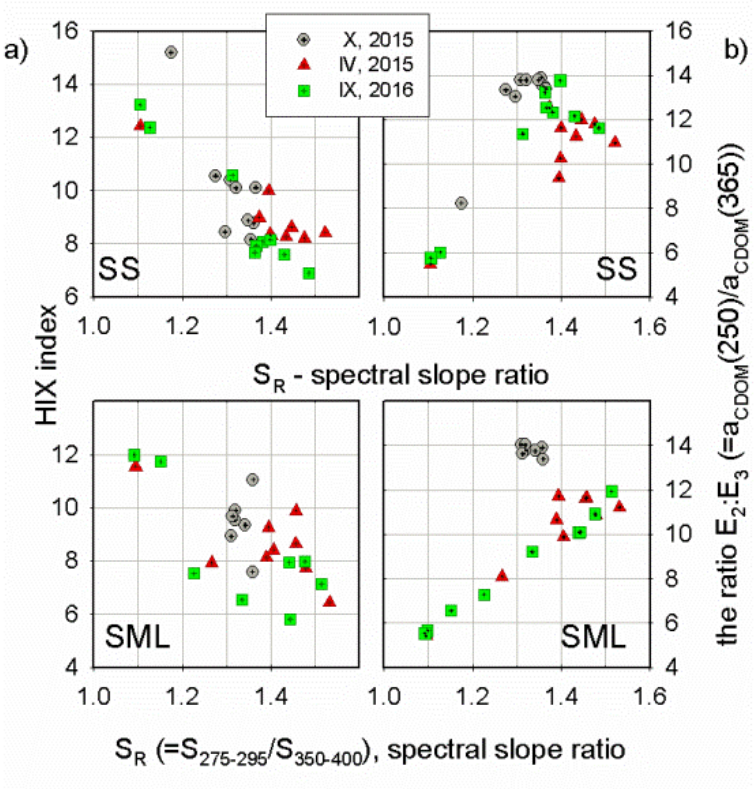


**Figure 9. The relationship between the spectral slope ratio, $S_R$, and (a) HIX index and (b) the ratio $E_2$:$E_3$ - for SS (top panels) and SML (bottom panels).**

**4. Discussion**

The values of the absorption coefficient, $a_{CDOM}(\lambda)$ show that with an increase of a distance from the river outlet, the intensity of light absorption (a proxy of amount of organic matter) is decreasing significantly, both in SML and SS. It shows that the main source of CDOM in the study area is the Vistula River. Additionally, the differences between the absorption values for SML and SS become smaller and smaller. The analysis of several absorption indices (S, $S_R$ and $E_2$:$E_3$) may reveal the changes in composition and a decrease in molecular weight of organic matter with an increase of salinity and a distance from the mouth of the river. Molecules brought into the sea with the river waters, with increasing salinity (and time and the distance from the mouth of the river) undergo such processes as the dilution of the fresh waters in sea waters and the degradation of the organic particles, induced by solar radiation (photo-bleaching) and by bacterial activity (biodegradation). The increase of S and $S_R$ and $E_2$:$E_3$ (a proxy of a decrease of molecular weight, MW) with salinity suggest a transfer of colored material from HMW fraction to the LMW fraction. Moreover, the linear regression coefficients for the relations between salinity and: S, $S_R$ and $E_2$:$E_3$ achieved higher values for SML than SS. The values of the linear regression coefficients can illustrate a rate of the breakdown of large molecules to smaller ones (HMW to LMW). They achieve the higher values in SML than in SS, thus show that in SML the processes occur faster than in SS. Furthermore, the values of S, $S_R$ and MW, are smaller in a vicinity of the river outlet about 2-, 0.5- and 3-times, respectively, than in open sea depict a presence of higher molecular weighted molecules in the estuarine waters, both in SML and SS. Hence, the higher values of $S_R$ indicate an increase of absorption in a short wavelength range (via an increase in concentration of low-weighted molecules, LWM) and a decrease of absorption in a longer wavelength range (a decrease in the concentration of big and more condensed and high-weighted molecules, HWM). However, in a vicinity of the river mouth (W1), the studied absorption indices reached the lower values in SML than in SS. It suggests that the molecules with large molecular mass predominate in a surface microlayer. Such results may be caused by the presence of the surface slicks, visible by a naked eye, made of big surface molecular structures. A riverine water brings into the sea a huge amount of the terrestrial amphiphilic (the molecules with hydrophobic and hydrophilic heads) organic molecules that form the surface slicks and despite the large weight of the surface molecular structures their hydrophobic properties make them float on the sea surface.

The spectrofluorometric studies complete and confirm the absorption studies. Wherein the concentration of components A, C, M and T were higher in SML than in SS in both coastal zone and open sea; the contribution of A and C components in FDOM composition decreased, while M and T increased, with an increase of salinity. Moreover, the values of the fluorescence intensity of FDOM components change linearly with salinity and the linear regression coefficients show higher values in SML than in SS. This may confirm a higher rate of the degradation processes occurring in SML. The relative changes of percentage contribution of FDOM components, with an increase of salinity, depict that a component which quantity varies the most, is a fluorophore T. It may indicate on production of protein-like fluorophores caused by photobleaching and biological activity. Additionally the results of the FDOM measurements indicate that FDOM concentration is about 2-3 times higher in the coastal zone (salinity <7) than in the open sea (> 7). The results of FDOM concentration indicate the dominance of terrestrial molecules (allochthonous) in estuarine waters - due to high concentration of molecules brought by a river (A and C). The ratio (M+T)/(A+C) increased with salinity and reached the highest values in the open sea: 0.79 and 0.63 in SML and SS, respectively. Photo-degradation effect, induced by solar radiation on the molecules in a sea surface layer, results in degradation

of macromolecules into particles with a lower molecular weight (i.e., a decrease of A and C and the increase the amount of molecules of lower molecular weight produced in the sea (M and T) and this process acts more rapidly in SML, (Fig. 8). The above conclusion is confirmed by the results of the ratio (M+T)/(A+C) and HIX index, which achieve respective higher and lower values in the SML than in SS due to higher fluorescence intensity at a short wavelength band belonging to marine FDOM components (M and T). The elevated values of HIX in the SS are an evidence of a more advance humification process of the organic molecules that make the organic molecules more condensed and with higher aromaticy.

## 5. Conclusions

The results of the studies on the absorption and fluorescence properties of the organic matter included in the SML and SS waters are complementary. The values of the absorption coefficients as well as the fluorescence intensity give information about the decline in the CDOM/FDOM concentration with increasing salinity, both in SS and SML. ~~What is more~~ Moreover, a decreasing of DOM concentration with salinity occurs faster in SML than in SS. Analysis of absorption and fluorescence spectra allow the detection of subtle changes in the percentage composition of CDOM/FDOM components that revealed an increase of M and T (produced in-situ, in the sea) and a simultaneous decrease in A and C (terrestrial origin) with increasing salinity. Moreover the changes of the percentage composition occur in SML more rapidly than in SS. The results suggest a higher rate of degradation processes in a surface microlayer

In addition, the analysis of indices obtained from the values of the intensity of the absorption and fluorescence of the samples enabled tracking sources and processes, which have been subjected to investigated molecules, in SML and SS. The authors: (i) confirm that the processes of structural changes in molecules of HMW to LMW, due to effects of photo- and biodegradation, occur faster in SML than in SS; (ii) organic molecules contained in a surface microlayer, SML, have a smaller molecular mass than SS, thus, SML and SS are characterized by different percentage distributions of the main FDOM components; (iii) the fresh water of the Vistula River is the main driving force of allochthonous character of organic matter in coastal waters of Gulf of Gdansk.

Summarizing, the distributions of light intensity reached over or behind the sea surface is modified effectively by the specific absorption and/or emission of a light by surfactants. The degradation processes of the organic molecules contained in SML and SS proceed at different rates. Hence, the DOM molecules included in the SML can specifically modify the physical processes associated with the sea surface layer. It should be necessary to continue a study on the physical properties of surface microlayer in other Baltic Sea sites and in less urbanized and more natural and pristine region, like Arctic.

## Acknowledgment

The work described in this paper was supported by a grant of ESA (European Space Agency) OCEAN FLUX, No 502-D14IN010. We also acknowledge the support by the funds of the Leading National Research Centre (KNOW) received by the Centre for Polar Studies for the period 2014-2018.

**References**


Blough N.V., S.A. Green, 1995, Spectroscopic characterization and remote sensing of nonliving organic matter. p. 23– 45 *In* R. G. Zepp and C. Sonntag [eds.], Role of nonliving organic matter in the earth's carbon cycle. Wiley.

Bracchini L., A.M. Dattilo, ,S.A. Loiselle, A. Cozar, A. Tognazzi, N. Azza, C. Rossi, 2006, The role of wetlands in the chromophoric dissolved organic matter release and its relation to aquatic ecosystems optical properties. A case of study: Katonga and Bunjako Bays (Lake Victoria, Uganda). Chemosphere 63: 1170–1178.

Brown M, 1977, Transmission spectroscopy examinations of natural waters, Estuar. Coast. Mar. Sci. 5: 309–317.

Carder K.L., R.G. Steward, G.R. Harvey, P.B. Ortner, 1989, Marine humic and fulvic acids: Their effects on remote sensing of ocean chlorophyll. Limnol. Oceanogr. 34: 68–81.

Chari N.V.H.K., N.S. Sarma, S.R. Pandi, K.N. Murthy, 2012, Seasonal and spatial constraints of fluorophores in the midwestern Bay of Bengal by PARAFAC analysis of excitation emission matrix spectra, Estuarine, Coastal and Shelf Science 100 (2012), 162-171, DOI: 10.1016/j.ecss.2012.01.012.

Chen H., B. Zheng, J. Song, Y. Qin, 2011, Correlation between molecular absorption spectral slope ratios and fluorescence humification indices in characterizing CDOM, Aquat Sci, 73: 103-112, DOI 10.1007/s00027-010-0164-5.

Chin Y. -P., G. Aiken, E.O. Loughlin, 1994, Molecular weight, polydispersity, and spectroscopic properties of aquatic humic substances, Environ. Sci. Technol. 28, 1853–1858.

Coble P., 1996, Characterization of marine and terrestrial DOM in seawater using excitation-emission matrix spectroscopy, Marine Chem. 51, 325-346.

Coble P., 2007, Marine optical biogeochemistry: the chemistry of ocean color, Chemical Reviews. 107**,** 402-418.

Ćosović B., V. Vojvodić, 1998, Voltammetric Analysis of Surface Active Substances in Natural Seawater, Electroanal. 10, 429-434.

Cunliffe M.A., S. Engel, S. Frka, B. Gašparović, C. Guitart, J. C. Murrell, M. Salter, C. Stolle, R. Upstill-Goddard, O. Wurl, 2013, Sea surface microlayers: A unified physicochemical and biological perspective of the air–ocean interface, Prog. Oceanogr. 109, 104-116.

De Haan H., T. De Boer, 1987, Applicability of light absorbance and fluorescence as measures of concentration and molecular size of dissolved organic carbon in humic Laken Tjeukemeer. Water Res. 21: 731–734.

Natural water fluorescence characteristics based on the lidar investigations of the water surface layer, Oceanologia , no.44(3), pp.339-354.

Drozdowska V., M. Józefowicz, 2015, Spectroscopic studies of marine surfactants in the southern Baltic Sea, Oceanol. 57, 159-167 (2015).

Drozdowska V., P. Kowalczuk, M. Józefowicz, 2015, Spectrofluorometric characteristics of fluorescent Rapid 10, 15050, doi: 10.2971/jeos.2015.15050.

Drozdowska V., W. Freda, E. Baszanowska, K. Rudź, M. Darecki, J. R. Heldt, H. Toczek, 2013, Spectral properties of natural and oil polluted Baltic seawater – results of measurements and modeling, Eur. Phys. J. Special Topics 222, 1-14.

Garrett W. D., 1965, Collection of slick-forming materials from the sea surface, Limnol Oceanogr. 10, 602–605.

Glatzel S., K. Kalbitz, M. Dalva, T. Moore, 2003, Dissolved organic matter properties and their relationship to carbon dioxide efflux from restored peat bogs, Geoderm. 113, 397–411.

Guéguen, C., L. Guo, M. Yamamoto-Kawai, N. Tanaka, 2007, Colored dissolved organic matter dynamics across the shelf/basin interfaces in the western Arctic Ocean. Journal of Geophysical Research 112, C05038.

Helms J.R., A. Stubbins, J.D. Ritchie, E.C. Minor, D.J. Kieber, K. Mopper, 2008, Absorption spectral slopes and slope ratios as indicators of molecular weight, source, and photobleaching of chromophoric dissolved organic matter. Limn Oceanogr 53:955–969.

Hudson N., A. Baker, D. Reynolds, 2007, Fluorescence analysis of dissolved organic matter in natural, waste and polluted waters—a review, River Research and Appl. 23, 631-649.

Jørgensen, L., C.A. Stedmon, T. Kragh, S. Markager, M. Middelboe, M. Søndergaardv, 2011, Global trends in the fluorescence characteristics and distribution of marine dissolved organic matter. Marine Chemistry 126, 139e148.

Kowalczuk P., J. Ston-Egiert, W.J. Cooper, R.F. Whitehead, M.J. Durako, 2005, Characterization of chromophoric dissolved organic matter (CDOM) in the Baltic Sea by excitation emission matrix fluorescence spectroscopy, Marine Chem. 96, 273--292.

Kowalczuk, P., M. Zabłocka, S. Sagan, K. Kuliński, 2010, Fluorescence measured in situ as a proxy of CDOM absorption and DOC concentration in the Baltic Sea. Oceanologia 52, 431-471.

Lakowicz J.R., 2006, Principles of fluorescence spectroscopy, third edition. Plenum Press: New York, 2006.

Liss P.S., R.A. Duce, 2005, The Sea Surface and Global Change, Cambridge University Press, 2005.

Liss P.S., A.J. Watson, E.J. Bock, B. Jahne, W.E. Asher, N.M. Frew, L. Hasse. G.M. Korenowski, L. Merlivat, L.F. Phillips, P. Schlussel, D.K. Woolf, 1997, Report Group I – Physical processes in the microlayer and the ait-sea exchange of trace gases. In: The Sea Surface and Global Change, P.S. Liss, R.A. Duce, Edss., Cambridge University Press, UK, 1-34.

Loiselle S.A., L. Bracchini, A.M. Dattilo, M. Ricci, A. Tognazzi, A.Co´zar, C. Rossi, 2009, The optical characterization of chromophoric dissolved organic matter using wavelength distribution of absorption spectral slopes. Limnol Oceanogr 54:590–597.

Maciejewska A., J. Pempkowiak, 2015, DOC and POC in the southern Baltic Sea. Part II – Evaluation of factors affecting organic matter concentrations using multivariate statistical methods, Oceanol., 57, 168–176.

McKnight D.M., R. Harnisch, R.L. Wershaw, J.S. Baron, S. Schiff, 1997, Chemical characteristics of particulate, colloidal, and dissolved organic matter in Loch Vale Watershed, Rocky Mountain National Park, Biogeochem. 36, 99–214.

Milori D., L. Martin-Neto, C. Bayer, J. Mielniczuk, V. Vagnato, 2002, Humification degree of soil humic acids determined by fluorescence spectroscopy, Soil Sci. 167, 739–749; DOI: 10.1097/01.ss.0000038066.07412.9c.

Moran M.A., W.M. Sheldon, Jr., R.G. Zepp, 2000, Carbon loss and optical property changes during long-term photochemical and biological degradation of estuarine dissolved organic matter, Limnol. Oceanogr., 45(6), 1254–1264.

Murphy K.R., K.D. Butler, R.G.M. Spencer, C.A. Stedmon, J.R. Boehme, G.R. Aiken, 2010, Measurement of Dissolved Organic Matter Fluorescence in Aquatic Environments: An Interlaboratory Comparison, Environ. Sci. Technol., 44, 9405–9412.

Ostrowska M., Darecki M., Krężel A., Ficek D., Furmańczyk K., 2015, Practical applicability and preliminary results of the Baltic Environmental Satellite Remote Sensing System (SatBałtyk), Polish Maritime Research, ISSN 1233-2585, 3(87), 22, 43-49

Parlanti E., K. Wo¨rz, L. Geoffroy, M. Lamotte, 2000, Dissolved organic matter fluorescence spectroscopy as a tool to estimate biological activity in a coastal zone submitted to anthropogenic inputs, Organic Geochem. 31(12), 1765–1781.

Petelski T., P. Markuszewski, P. Makuch, A. Jankowski, A. Rozwadowska, 2014, Studies of vertical coarse aerosol fluxes in the boundary layer over the Baltic Sea, Oceanol., 56(4), 697-710, doi:10.5697/oc.56-4.697

Peuravouri J., K. Pihlaja, 1997, Molecular size distribution and spectroscopic properties of aquatic humic substances. Anal. Chim. Acta 337: 133–149.

Sarpal R.S, K. Mopper, D.J. Keiber, 1995, Absorbance properties of dissolved organic matter in Antarctic sea water, Antarc. J. 30: 139–140.

Soloviev A, R. Lukas, 2006, Near-surface layer of the ocean, Structure, dynamics and applications, Springer, 2006.

Stedmon C.A., S. Markager, R. Bro, 2003, Tracing dissolved organic matter in aquatic environments using a new approach to fluorescence spectroscopy. Mar. Chem. 82: 239–254, DOI:10.1016/S0304-4203(03)00072-0.

Summers R.S., P.K. Cornel, P.V. Roberts, 1987, Molecular size distribution and spectroscopic characterization of humic substances, Sco. Tot. Environ., 62, 27-37.

Uścinowicz S., 2011, Geochemistry of Baltic Sea, Surface sediments, Sci.Eds. S. Uścinowicz, PIG-PIB, Warsaw, 2011).

Vaishaya A., S.G.Jennings, C. O'Dowd, 2012, Wind-driven influences on aerosol light scattering in north-east Atlantic air, Geoh. Res. Let., 39, DOI:10.1029/2011GL050556.

Williams C.J., Y. Yamashita, H.F. Wilson, R. Jaffe´, M.A. Xenopoulos, 2010, Unraveling the role of land use and microbial activity in shaping dissolved organic matter characteristics in stream ecosystems, Limnol. Oceanogr., 55(3), 1159–1171.

Zhang Y, M.A. van Dijk, M. Liu, G. Zhu, B. Qin, 2009, The contribution of phytoplankton degradation to chromophoric dissolved organic matter (CDOM) in eutrophic shallow lakes: Field and experimental evidence. Water Res 43:4685–4697.

Zhang Y., X. Liu, C.L. Osburn, M. Wang, B. Qin, Y. Zhou, 2013, Photobleaching Response of Different Sources of Chromophoric Dissolved Organic Matter Exposed to Natural Solar Radiation Using Absorption and Excitation–Emission Matrix Spectra, PLOS ONE, 8 (10), e77515, 1-14.

Zsolnay A., E. Baigar, M. Jimnez, B. Steinweg, F. Saccomandi, 1999, Differentiating with fluorescence spectroscopy the sources of dissolved organic matter in soils subjected to drying, Chemosph. 38, 45–50.